INVESTIGATION OF EQUILIBRIUM, GLOBAL MODES AND MICROINSTABILITIES IN THE STELLARATOR W7-AS

A. WELLER, M. ANTON, R. BRAKEL, J. GEIGER, C. GÖRNER, H.J. HARTFUSS,
M. HIRSCH, R. JAENICKE, C. NÜHRENBERG, S.D. PINCHES,
D.A. SPONG[1], S. ZOLETNIK[2], W7-AS TEAM, NBI- and ECRH GROUP[3]

Max-Planck-Institut für Plasmaphysik
IPP-EURATOM-Association
D-85748 Garching, Germany

Abstract

Equilibrium and stability properties in the WENDELSTEIN 7-AS stellarator are investigated experimentally and compared with theoretical predictions for particular cases. The topology of equilibrium magnetic surfaces and of global MHD modes is inferred from X-ray tomography. The predicted effects of externally driven currents and internal currents on the equilibrium surfaces could be confirmed experimentally. In particular the reduced Shafranov shift due to reduced Pfirsch-Schlüter currents in W7-AS could be verified. Up to the maximum accessible β ($\langle\beta\rangle \approx 2\%$) plasmas can be confined without significant deterioration by pressure driven MHD-activity. However, global modes in the stable MHD spectrum such as global and toroidal Alfvén eigenmodes (GAE, TAE) can be destabilised by energetic ions from neutral beam heating. These instabilities appear as very coherent low frequency modes (≤ 40 kHz) in the lower β regime without significant impact on the global confinement. At medium β very strong particle driven MHD modes with frequencies up to the range of 500 kHz can be observed. These modes can show nonlinear behaviour including periodic bursting and frequency chirping in combination with significant plasma energy losses. With increasing β Alfvén modes are widely stable, because under these conditions the damping relative to the particle drive is increased. Besides the global mode activity small scale turbulent structures have been investigated in the plasma core and at the edge. The measured data of electron temperature, density and magnetic fluctuations do not yet allow to assess turbulence driven transport fluxes. However, correlations with the global confinement have been found, and the measured amplitudes are in the range expected to be relevant for anomalous transport. The observed dependence of the confinement on the edge rotational transform and magnetic shear can be explained in terms of enhanced transport at rational surfaces, however, the underlying mechanism is still unclear.

1. INTRODUCTION

In WENDELSTEIN 7-AS (major radius R = 2 m, effective plasma radius a ≤ 0.2 m) the magnetic configuration has been optimised to some extent with respect to equilibrium, MHD stability and neoclassical transport properties. A key element is the reduction of the internal parallel currents (Pfirsch-Schlüter and bootstrap currents) achieved by a 3-dimensional field geometry, which results in good equilibrium properties (eg. small Shafranov shift) and improved MHD stability simultaneously [1]. The existence of high quality flux surfaces is the basis for good confinement in W7-AS. In the usual net-current-free operation the configuration is characterised by very low magnetic shear, and therefore, small field errors can lead to large stationary islands particularly around low order rational surfaces. Since also MHD instabilities as well as magnetic turbulence are expected to lead to deteriorations of a similar kind, the rotational transform $\iota = 1/q$ is adjusted by means of the toroidal field system to avoid major resonances. Optimum confinement is established when ι stays within nearly resonance-free zones just in the vicinity of 1/3 and 1/2. Detailed measurements of vacuum flux surfaces using a probing electron beam [1,2] have shown both, a good agreement with field line tracing calculations as well as the existence of large islands, if low order resonances are contained in the ι-profile. In the presence of plasma the surfaces are modified by the internal currents. The edge rotational transform can be feedback

---

controlled by driving a small Ohmic heating (OH) current, which compensates the bootstrap current (net current-free operation). Current driven MHD such as tearing modes only occurs in the presence of significant net currents driven inductively or by electron cyclotron current drive (ECCD) [3]. In the absence of significant magnetic shear the global MHD stability against pressure driven modes (interchange and ballooning modes) relies on a magnetic well. The predicted ideal MHD stability limits for standard field configurations in W7-AS are in the range $\langle\beta\rangle \approx 2$ %. A main purpose of this paper is the attempt to benchmark the predicted MHD properties with experimental data. Another related aim is to investigate the interrelation of global MHD activity and small scale turbulent fluctuations with anomalous transport, confinement transitions and operational limits. A particular emphasis is on Alfvén Eigenmodes, which are in the stable MHD spectrum, but which can be destabilised by resonant Landau interactions with energetic ions from neutral beam injection (NBI). These modes cannot be easily suppressed by field optimisation, and therefore, their role needs to be further investigated in devices like W7-X.

2. HIGH-BETA EQUILIBRIUM AND MHD MODES

Maximum β values of $\langle\beta\rangle \approx 1.9$ % and $\beta(0) \approx 4.5$ % have been reached in W7-AS at magnetic fields of B = 0.9 - 1.3 T with NBI heating powers up to 3 MW [4]. The almost tangential injection system operates at 50 - 55 kV and allows for balanced injection, in order to avoid too large beam driven currents. Under the conditions of high β the electron density reaches $2-3\times10^{20}$ m^{-3} leading to temperatures of only 200 - 300 eV.

The reconstruction of equilibrium surfaces by magnetic probe measurements in W7-AS is very difficult due to the small field changes. Therefore, a multi-camera soft X-ray detector system was installed for tomographic analyses of equilibrium surfaces and mode structures [5,6]. This device consists of 10 compact cameras with a total number of 320 sight-lines surrounding the plasma inside the vacuum vessel. Various numerical methods for the reconstruction of the emissivity contours and for the separation of mode structures from the equilibrium have been applied.

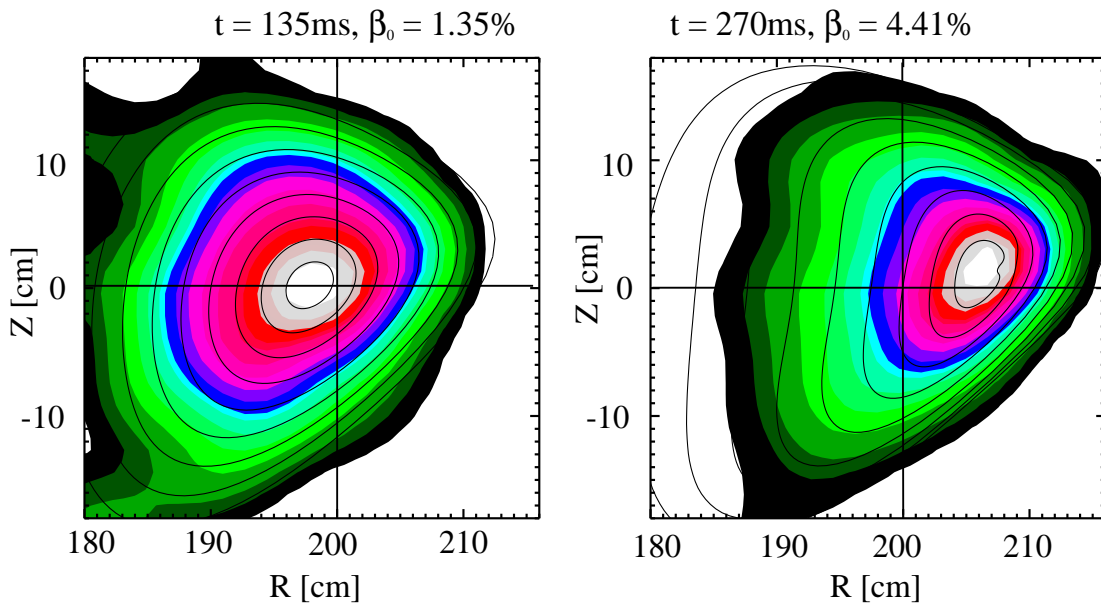$t = 135\text{ms}, \beta_0 = 1.35\%$　　　　$t = 270\text{ms}, \beta_0 = 4.41\%$

Fig. 1. X-ray emissivity contours as obtained from tomographic reconstructions (Maximum Entropy method) compared with equilibrium flux surfaces (NEMEC code, solid contour lines). The analysis is made for the low-β phase (left, β(0) ≈ 1.4 %) and the high-β phase (right, β(0) ≈ 4.4 %) of #41618. The β induced horizontal axis shift reaches 7 - 8 cm.

A particular aim was to compare the NEMEC free boundary equilibrium code calculations [7] with experimental data. The calculated equilibria are widely used for plasma analysis. Very good agreement is usually obtained between the equilibrium calculations and X-ray tomographic reconstructions, particularly in the gradient region of the X-ray emissivity profiles, where the reconstructions are most reliable. Two major effects predicted by the code calculations could be verified: - firstly, the displacement of the flux surfaces due to Pfirsch-Schlüter currents (Shafranov shift) in agreement with earlier measurements [2], - secondly the different modification of flux

surfaces by parallel and antiparallel inductive currents [7]. The effect of the Shafranov shift is illustrated in fig. 1 where X-ray tomograms at different β during a discharge are compared with NEMEC calculations. In accordance with the calculations the observed horizontal axis shift at high β (β(0) ≈ 4.5 %) reaches values, which correspond to a significant fraction of the plasma radius (0.4 - 0.45 a). Along with the geometric changes of the flux surfaces the ι-profile is modified from $\iota \approx 0.35$ (almost constant in vacuum configuration) to a moderate shear profile at high β that varies between $0.404 \geq \iota \geq 0.27$ between center and edge. Therefore, at high β low order rational surfaces cannot be avoided anymore.

Actually under these conditions often coherent low frequency (≈ 4 kHz) mode activity is observed in the X-ray emission, which indicates a pressure driven global mode at the most important rational surface. In addition weak MHD activity is found around 15 and 35 kHz, which is probably driven by fast particles (see section 3.). For the same discharge, which was used for the equilibrium analysis shown in fig. 1, a stability analysis has been performed for the high-β case (#41618, B = 1.22 T, $\langle \beta \rangle$ = 1.7 %, β(0) = 3.6 %, $n_e = 1.8 \times 10^{20}$ m^{-3}, T_e = 0.35 keV, P_{NBI} ≈ 3 MW). The local analysis comprised the evaluation of the local stability criteria (Mercier criterion, resistive interchange criterion), and the local ballooning analysis along a closed field line [8]. The Mercier criterion indicates stability across the whole plasma, whereas the resistive interchange criterion is violated for s ≥ 0.75 (s normalised flux coordinate), which corresponds to an effective plasma radius of r ≈ 15.25 cm. This is consistent with an earlier study of configurations with reduced magnetic well [9]. The evaluation of the local stability analysis is shown in fig. 2. The field line ballooning indicates also stability in the outer plasma region, for example at the rational surfaces ι = 3/10 at s = 0.688 and ι = 2/7 at s = 0.818.
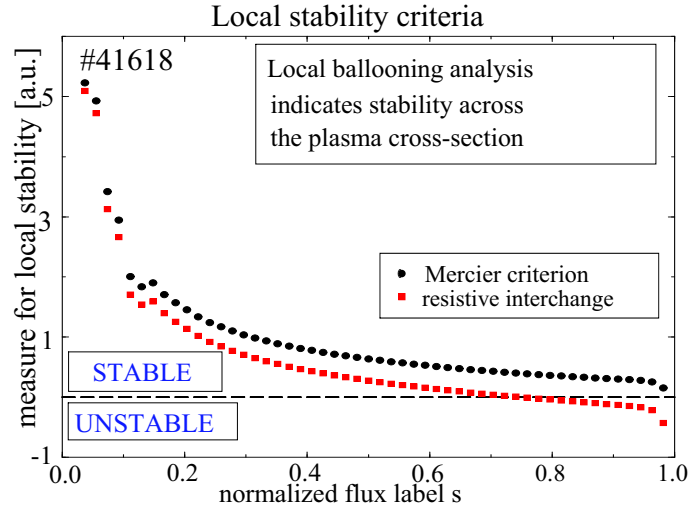

Fig. 2. The local stability analysis of the high-β shot 41618 yields a resistive-interchange unstable region for s ≥ 0.75 (r ≥ 15.25 cm). The plasma is ideally stable across the whole plasma.

The global stability properties have been studied with the CAS3D code [10,11]. The latest code version (CAS3D3) [12] also allows to analyse the stable part of the ideal MHD spectrum in full three-dimensional (3-d) geometry, including fluid compression and using a physical kinetic energy term, so that physical growth rates and frequencies can be calculated for comparison with measured frequencies. In the analysis 162 radial intervals and 40 perturbation Fourier harmonics have been used, which were selected according to the ι-profile and the mode family chosen (N = 0,1,2 in the 5-periodic W7-AS) [10]. In the stable MHD spectrum the computational spectra for the N = 1 and N = 2 mode families, which have been studied in more detail, show gap formation, which may occur in the sound spectrum as well as in the Alfvén spectrum. Several gap modes in the CAS3D3 calculations have been detected by comparisons with the analytical sound and Alfvén continua: in the low frequency part several global modes (N = 1) appear in a toroidicity and an ellipticity induced gap of the sound spectrum, respectively ((m,n) = (3,1) + (4,1) at ≈ 1.8 kHz, and (4,1) + (2,1) at ≈ 4.6 kHz), where m,n are the poloidal and toroidal mode numbers). In the higher frequency range the CAS3D3 calculations reveal gap formation in the Alfvén branches of the spectrum and the existence of global, stable modes. In particular, toroidal Alfvén eigenmodes (TAE) with main components (m,n) = (3,1) + (4,1) (N = 1

mode family) at 22 kHz and $(m,n) = (6,2) + (7,2)$ (N = 2 mode family) at 38 kHz are predicted. Typically several global modes are found by CAS3D3, which are composed of similar poloidal mode numbers, but differ in the number of radial nodes and in the sign of the poloidal harmonics (odd and even modes). The global modes may be destabilised by resonant fast particles (see next section) and cause some of the experimentally observed activity. However, more computational and experimental studies are needed to explain this weak MHD-activity in the high-β regime.

3. ENERGETIC PARTICLE DRIVEN MODES

The most striking MHD instabilities in W7-AS have been identified as global Alfvén eigenmodes, which are in the stable MHD spectrum driven unstable by wave particle resonances with energetic ions of the neutral beam slowing down distribution [13]. These modes cannot be suppressed by avoiding rational surfaces since they occur in gaps of the continuous shear Alfvén spectrum given by $\omega_A = k_\parallel \cdot v_A$ with finite parallel wave vector $k_\parallel \equiv (m \cdot \iota - n)/R \neq 0$. Under the usual low shear conditions in W7-AS and close to a low order resonance $\iota = n/m$, where optimum confinement is found [14], the (m,n) continuum does not extend to zero frequency. Underneath the continuous spectrum a gap remains, in which global Alfvén eigenmodes (GAE) with low frequencies are predicted (typically 20 - 40 kHz in W7-AS) [13,15]. Experimentally they appear typically as coherent mode activity with one or a few lines dominating the frequency spectrum. This activity is usually not causing any significant transport. The spatial 2-d structure of GAE and TAE modes has been derived from X-ray tomography analysis.
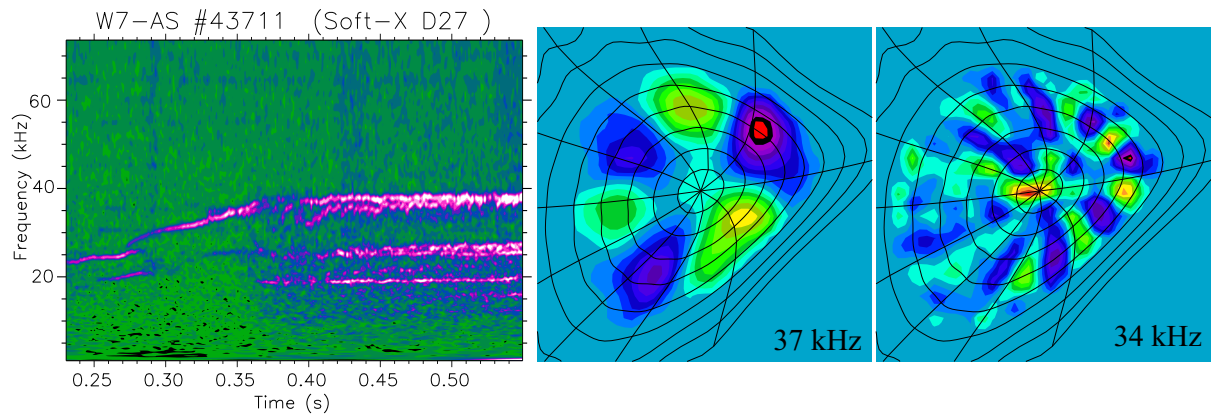

Fig. 3. GAE-activity in a HNBI discharge. In the frequency spectrogram of a soft X-ray signal several lines appear below 40 kHz (left). For the upper 2 lines the X-ray reconstructions show extended mode structures with m = 3 (middle) and with higher (m = 8,9, or 10?, right).

In fig. 3 an example is shown for a more complicated frequency spectrum (left) and for reconstructed mode structures (right) corresponding to the 2 uppermost spectral lines. Whereas in the case of the equilibrium reconstructions the maximum entropy method is used, a first order regularisation method is used for the mode analysis in combination with either Fourier filtering of the raw data or singular value decomposition (SVD) techniques in order to separate different mode structures [5]. The analysis of fig. 3 refers to a high-confinement NBI discharge (HNBI) in W7-AS [16] (#43711, B = 2.5 T, $n_e = 1 \times 10^{20}$ m^{-3}, $T_e = 0.9$ keV, $P_{NBI} \approx 0.35$ MW). In this case a relatively high bootstrap current develops, which is compensated by an OH-current, resulting in the formation of $\iota = 1/3$ in the plasma, therefore, closing of the (3,1) gap towards the plasma center. In many cases modes with a similar poloidal structure are observed, which are at different frequencies, and also differ by a node in their radial eigenfunctions.
The influence of (moderate) magnetic shear on the Alfvén spectrum has been studied by driving OH-currents of different magnitude and polarity [17]. With increasing shear a transition from GAE to TAE modes has been found. A TAE mode has been identified in discharge #39042 by the poloidal structure, which varies from m = 6 in the outer region to m = 5 towards the inside as deduced from the X-ray tomographic analysis (fig. 4). The mode structure and frequency are in agreement with CAS3D3 code calculations. Additional (axisymmetric) calculations with a TAE/GAE gyrofluid model [15], which includes drive and damping terms to describe the particle effects, give similar results and predict instability for the n = 2 (m =5,6) TAE mode observed.
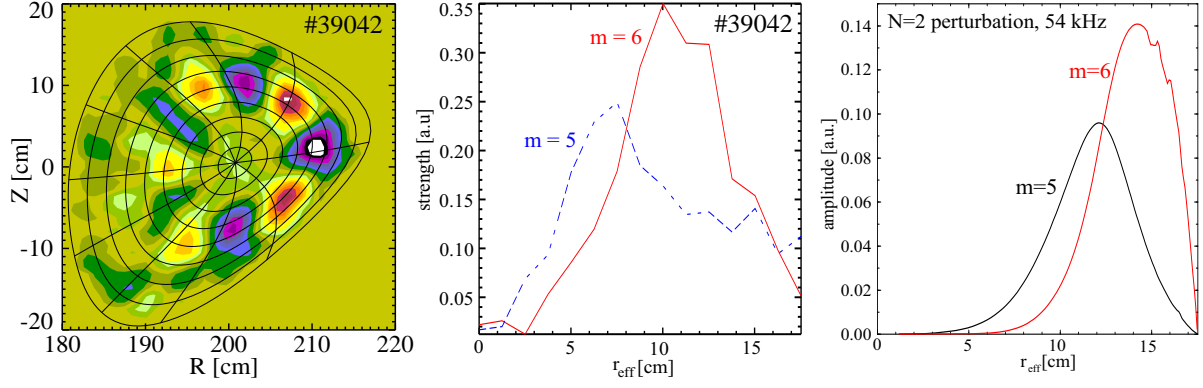
Fig. 4. X-ray tomography of a TAE mode with main poloidal components m = 6 outside and m = 5 inside (left). In the middle radial profiles of the two main poloidal harmonics from Fourier decomposition of the tomogram are shown, which are in qualitative agreement with the Fourier harmonics of the normal displacement as calculated with CAS3D3 (right).

For the case of this (weak) TAE activity the interaction of the mode with the fast particles has been studied with the guiding center particle following code HAGIS [18]. As input toroidal averages of the equilibrium and of the perturbations from CAS3D3 (fig. 4, right), as well as calculated radial and energy distributions of the particles were used. A saturation amplitude of $\tilde{B}/B \approx 2 \times 10^{-4}$ and a linear growth rate for the particle drive of $\gamma/\omega \approx 1.5\,\%$ has been calculated, which is consistent with typical gyrofluid calculations. The particle interaction with the TAE causes a 15 % shift of the MHD frequency and very small redistributions of the fast particle distributions around the resonances ($\approx 10^{-4}$ relative density perturbation), which, however, do not lead to any significant particle losses.

The low frequency coherent GAE modes occur preferentially in the low-β NBI regime (low shear, $n_e(0) \approx 10^{-20}$ m^{-3}, low NBI power), where the Alfvén speed typically exceeds the fast ion velocity. Therefore, the modes with poloidal wave number m are excited via the m $\pm$ 1 sideband resonances at much lower resonant particle velocities (typically $v_{\parallel,m+1} \approx 0.1 \cdot v_A$) if the ι-profile is close to the rational value n/m (small $k_{\parallel}$). This is sketched in fig. 5, where the resonant particle velocities for fundamental and sideband excitation are compared as a function of mode number m.

Under conditions, where a significant fraction of fast particles has velocities $\geq v_A$ and the fast particle beta is sufficiently high, the beam driven mode activity can change significantly. A transition to higher frequencies (up to ≈ 500 kHz) and to bursting behaviour and intermittent
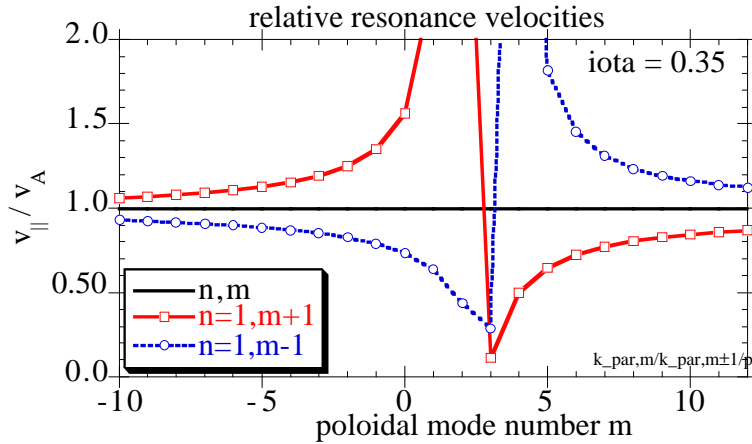

Fig. 5. Resonant parallel particle velocities normalised to the Alfvén speed for fundamental ($v_{\parallel} = v_A$) and m $\pm$ 1 sideband resonances. The rotational transform used (ι = 0.35) is close to n/m = 1/3. Under this condition the sideband resonance velocities for the (m,n) = (3,1) mode are well below v_A.
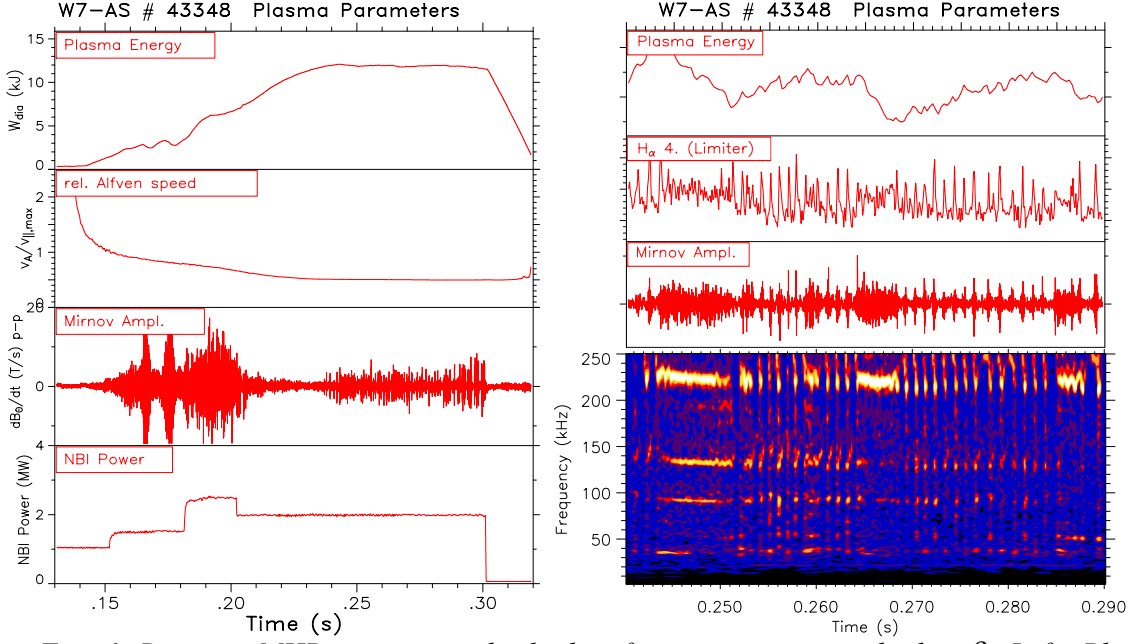
Fig. 6. Bursting MHD-activity in the higher frequency range at higher β. Left: Plasma energy (diamagnetic loop), averaged Alfvén speed normalised to maximum particle velocity, Mirnov signal and NBI power. Right: The mode activity is correlated with small relaxations of the plasma energy and H_α-emission. The Mirnov spectrogram shows several lines up to 250 kHz.

mode activity together with frequency chirping is often observed. This regime is characterised by relatively high β (low field) and intermediate NBI power, for which the plasma density can be kept well below the radiative density limit. This MHD activity can cause significant deterioration of the energy confinement as deduced from correlations with relaxations of the plasma energy and temperature. Inreased particle losses are deduced from the signature of the H_α-emission.
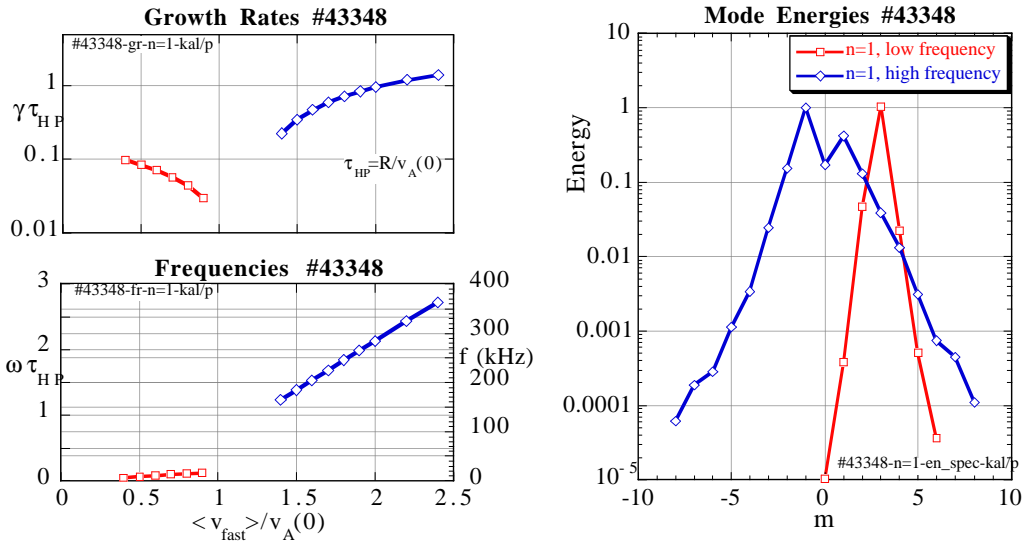

Fig. 7. Dependence of growth rates (upper left), frequencies (lower left) on the mean fast particle velocity normalised to the central Alfvén velocity as calculated with the parameters of #43348 (see fig. 6) by the gyrofluid model for the case n = 1. At higher velocities modes with significantly higher growth rates and frequencies are destabilised with much broader spectra of poloidal harmonics including opposite helicity modes (m < 0).

The bursting and frequency chirping behaviour suggests that at least a part of the lost particles could be fast ions resonating with the modes. In fig. 6 an example is shown for these effects (#43348, B = 1.2 T, $\langle \beta \rangle \approx 1.4$ %, $\beta(0) = 2.4$ %, $\beta_{fast}(0) \approx 0.5$ %, $n_e \approx 1.2 \times 10^{20}$ m^{-3}, $P_{NBI} \approx 2$ MW). The gyrofluid calculations for this case predict the transition to unstable Alfvén

modes in the frequency range of the observed activity as the mean fast particle velocity normalised to the central Alfvén speed exceeds unity (fig. 7). However, in the experiment $\langle v_{beam} \rangle / v_A(0)$ is marginally below 1. The higher threshold of the fast particle velocity in the calculations might be due to the approximation of the fast ion velocity distribution by a maxwellian. Compared with the low frequency GAE mode the calculated spectrum of poloidal mode harmonics in the case of the high frequency mode is broader and shifted to m numbers which involve higher $k_{\parallel}$-values.

The onset of the high frequency Alfvén modes is often observed during a density ramp, when v_A falls below the threshold for the fundamental resonance [19]. At higher densities approaching the maximum plasma β the beam driven modes usually become stabilised again, probably due to higher continuum damping (increased shear) and reduced values of $\beta_{fast}/\beta_{thermal}$. At the time of mode stabilisation a transition to better confinement is usually observed. A detailed understanding of the high frequency MHD activity is not possible so far due to lack of experimental data concerning the poloidal and radial structure. There might be also an explanation in terms of kinetic ballooning modes (KBM) or the energetic-particle continuum mode (EPM) [20,21]. The threshold condition to drive the EPM unstable given in ref. 19 is typically exceeded, but the expected frequency should be restricted to the range ≤ 80 kHz.

4. TURBULENCE AND FLUCTUATIONS

Under optimum confinement conditions the observed radial energy transport is reduced to neoclassical levels in a large interior region of the plasma [16,22]. In the majority of plasma conditions, however, anomalous transport plays an important role, in particular towards the plasma edge. Although MHD modes can cause enhanced transport, in most cases they cannot account for the anomalous transport, which is considered to be driven by microinstabilities. Small scale fluctuations are investigated by different diagnostics including an electron cyclotron emission (ECE) correlation radiometer, a reflectometer, μ-wave scattering, beam emission spectroscopy (BES) using a Lithium beam and magnetic probes. Due to the lack of measurements of electric field fluctuations inside the plasma no quantitative assessment of turbulent transport fluxes can be made at present. Here we try to describe the essential characteristics of the observed fluctuation and their interrelation with anomalous transport.
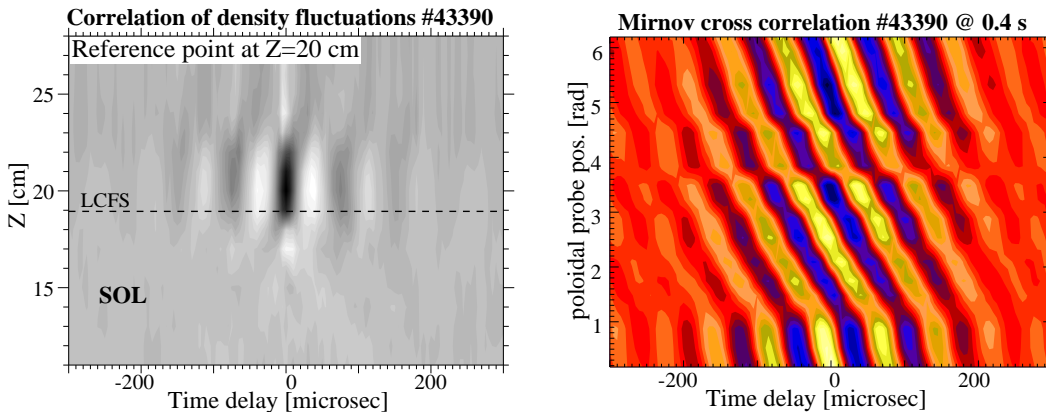

Fig. 8. Burst-like fluctuations inside the LCFS. Left: space-time correlation function of density fluctuations from BES. Right: poloidal correlation function of Mirnov signals.

The dependency of anomalous transport on details of the ɩ-profile (content of rational values and shear) [14] implies some features of the underlying turbulence: the instabilities are located around rational surfaces, and their effect is reduced by shear. These observations could be consistent with drift Alfvén turbulence [23], which also could provide a drive for Alfvén eigenmodes appearing occasionally during electron cyclotron heating (ECRH) or Ohmic heating [24] in the absence of fast ions. In the confinement region the turbulent electron temperature and density fluctuations in the 40 - 100 kHz range are in phase and well correlated. The temperature fluctuations [25] vanish under $\nabla T_e = 0$ conditions, where density fluctuations are still present. This behaviour could be explained by a convective mixing process which scales with $\tilde{T}_e / \nabla T_e$. The leading parameter dependency of the temperature fluctuations is an inverse scaling with the temperature.

A particular feature of the fluctuations at the edge is the burst-like oscillating instability extending over a few centimeters inside the last closed flux surface (LCFS) [26] well correlated in both density and magnetic signals. Fig. 8 shows the space-time correlation function of the density fluctuations as deduced from the Li-beam BES measurements and the cross correlation function for the poloidal array of 16 Mirnov coils. The Mirnov data imply rotating short-lived structures (50 - 100 μs) with $k_{\parallel}$-values of ≈ 0 and relatively long poloidal wavelengths in the range 30 - 50 cm. These burst-like fluctuations are considered to be related to transport because of their location, the scaling with density, the sensitive dependence on the ɩ-profile and their suppression during optimum confinement. Another class of fluctuations causing enhanced transport are ELM-like relaxations with typical duration of 200 - 500 μs, which can occur even outside the H-mode operational window [27]. As in the case of ELMs these relaxations cause a local flattening of the density and temperature profiles around the LCFS (particle and heat expulsion).

5. CONCLUSIONS

The predicted performance of the partially optimised stellarator configuration with respect to equilibrium flux surfaces and stability against pressure driven global modes at high β could be confirmed experimentally. The excitation of global Alfvén eigenmodes by resonant fast particles can lead to a significant deterioration of the confinement under particular operational conditions. Therefore, extensive experimental studies and numerical code calculations have been made in order to improve their understanding, which might help to assess their potential danger in larger machines like W7-X. Further studies, particularly in the higher frequency regime, seem to be necessary. The investigations of small scale fluctuations have shown correlations with anomalous transport. However, the underlying processes are not well known, and quantitative estimates of the turbulent transport are not possible on the basis of the available data.

REFERENCES

[1]   GRIEGER, G., et al., Phys. Fluids **B 4** (1992) 2081.
[2]   JAENICKE, R., et al., Nuclear Fusion **33** (1993) 687.
[3]   ERCKMANN, V., et al., these Proceedings.
[4]   WAGNER, F., et al., these Proceedings.
[5]   GÖRNER, C., et al., Proc. 24th EPS Conf. Berchtesgaden, **21A** Part IV (1997) 1625.
[6]   WELLER, A., et al., Proc. 12th Topical Conf. on High Temperature Plasma Diagn., Princeton 1998, to appear in Rev. of Sci. Instrum.
[7]   CALLAGHAN, H., et al., Proc. 24th EPS Conf. Berchtesgaden, **21A** Part IV (1997) 1617.
[8]   NÜHRENBERG, J. and ZILLE, R., in Theory of Fusion Plasmas, Varenna 1987, (Editrice Compositori, Bologna, 1988), EUR 11336 EN, p.3.
[9]   GEIGER, J., et al., Proc. 23rd EPS Conf. Kiev, **20C** Part II (1996) 491.
[10] SCHWAB, C., Phys. Fluids **B 5** (1993) 3195.
[11] NÜHRENBERG, C., Phys. Plasmas **3** (1996) 2401.
[12] NÜHRENBERG, C., submitted to Phys. Plasmas.
[13] WELLER, A., et al., Phys. Rev. Lett. **72** (1994) 1220.
[14] BRAKEL, R., et al., Proc. 25th EPS Conf. Prague (1998).
[15] SPONG, D.A., et al., Nuclear Fusion **35** (1995) 1687.
[16] STROTH, U., et al., Plasma Phys. Control. Fusion **40** (1998) 1551.
[17] GÖRNER, C., et al., Proc. 25th EPS Conf. Prague (1998).
[18] PINCHES, S.D., et al., Computer Physics Communication **111** (1998) 133.
[19] TEO, C.Y., et al., Nuclear Fusion **38** (1998) 409.
[20] TSAI, S.T. and CHEN, L., et al., Phys. Fluids **B 5** (1993) 3284.
[21] HEIDBRINK, W.W., Plasma Phys. Control. Fusion **37** (1995) 937.
[22] KICK, M., et al., Proc. 25th EPS Conf. Prague (1998).
[23] SCOTT, B., Plasma Phys. Control. Fusion **39** (1997) 1635.
[24] MARASCHEK, M. et al., Phys. Rev. Lett. **79** (1997) 4186.
[25] HARTFUß, H.J., et al., Plasma Phys. Control. Fusion **38** (1996) A221.
[26] ZOLETNIK, S., et al., submitted to Phys. Plasmas.
[27] HIRSCH, M., et al., Proc. 25th EPS Conf. Prague (1998).